Journal of Cleaner Production 220 (2019) 1014–1023

Contents lists available at ScienceDirect

Journal of Cleaner Production

journal homepage: www.elsevier.com/locate/jclepro

Exploring the association between the built environment and remotely sensed PM2.5 concentrations in urban areas

Man Yuan [a, b, *], Yan Song [c, **], Yaping Huang [a, b], Huanfeng Shen [d], Tongwen Li [d]

[a] School of Architecture and Urban Planning, Huazhong University of Science and Technology, Wuhan, China
[b] Hubei Engineering and Technology Research Center of Urbanization, Wuhan, China
[c] The Department of City and Regional Planning, The University of North Carolina at Chapel Hill, USA
[d] School of Resource and Environmental Science, Wuhan University, Wuhan, China

ARTICLE INFO

Article history:
Received 14 August 2018
Received in revised form
21 February 2019
Accepted 22 February 2019
Available online 23 February 2019

Keywords:
Air quality
Built environment
Remote sensing
Urban planning
China

ABSTRACT

Haze, especially $PM_{2.5}$, poses a serious threat to public health in China. $PM_{2.5}$ primarily originates from urban activities, and built environment may affect its formation and dispersion. Previous studies were based on limited data from ground-monitoring stations, and high resolution pollution maps are unavailable for statistical analyses. In this study, a 1 km*1 km wall-to-wall map of $PM_{2.5}$ concentration is developed with remote sensing data in Wuhan, China, and spatial statistics are used to figure out the influence of the built environment on $PM_{2.5}$ concentrations. In terms of land cover, high-rise high-density building areas have the largest impact on $PM_{2.5}$ concentrations, and the effect of forestland on the concentrations is not obvious in winter. In terms of land use, industrial lands are unrelated to air pollution in the downtown, while transportation has become a main source of $PM_{2.5}$ pollution. In terms of urban form, floor area ratio and building density are positively associated with $PM_{2.5}$ concentrations, and different types of road densities have different effects on air pollution. Finally, the implications of the study for urban planning and development are given. It is necessary to develop a polycentric urban structure to balance high population density and reduce traffic emissions in downtown areas. Road and bus networks should be optimized simultaneously to reduce traffic emissions and "small blocks and narrow roads" may be considered as an alternative for urban development. The spatial morphology of streets and buildings should be considered during urban design and urban renewal. In general, the study contributes to the application of remote sensing in urban planning and development, and remotely sensed $PM_{2.5}$ concentration data could provide further findings than the air pollution data obtained from ground monitoring and "bottom-up" models in past studies.

1. Introduction

Haze, also referred to as smoke fog, has become a serious environmental problem for cities across the globe, especially in developing countries such as China (Han et al., 2017) and others in South and Southeast Asia (Shi et al., 2018). Among air pollutants in haze, $PM_{2.5}$ (particulate matter in the air that is less than 2.5 μm in aerodynamic diameter) is a key pollutant affecting human health because it can deposit dangerous materials like heavy metals and sulfates in human respiratory tracts and lungs (Chen et al., 2017). Several studies have confirmed that exposure to $PM_{2.5}$ can lead to an increase in cardiovascular and respiratory diseases (Dominici et al., 2006), lung cancer (Han et al., 2017), and mortality (Laden et al., 2006). Increasing anthropogenic emissions driven by rapid urbanization have led to serious $PM_{2.5}$ pollution across China (Cao et al., 2011). For example, Beijing suffered more than 20 hazy days in January 2013, with the maximum hourly $PM_{2.5}$ concentration exceeding 600 $\mu g/m^3$ at this time (nearly 10 times the national air quality limit) (Wang et al., 2014). Various studies from different disciplines have focused on the scientific issues of formation, features and controlling strategies of $PM_{2.5}$ pollution in China, and these studies provided implications for the Chinese government and the public to address the challenge (Fu and Chen, 2017).

$PM_{2.5}$ predominantly originates from urban activities such as

* Corresponding author. School of Architecture and Urban Planning, Huazhong University of Science and Technology, Wuhan, China.
** Corresponding author.
E-mail addresses: yuanman_aup@hust.edu.cn (M. Yuan), ys@email.unc.edu (Y. Song).

https://doi.org/10.1016/j.jclepro.2019.02.236
0959-6526/

vehicle exhaust, coal and fuel combustion, dust from paved roads, and secondary sulfates (Pui et al., 2014). The process of using coal-reliant sources for heating and industrial activities has either been discontinued or technologically improved to decrease emissions, and pollutant loads from the coal and chemical industries have dramatically decreased in China. At the same time, the rising number of vehicles in Chinese cities, especially private cars, has made traffic-induced $PM_{2.5}$ the largest source of haze pollution (Liu and He, 2012). Besides ownership control and traffic restriction, some studies have shown that the built environment can affect concentrations of air pollutants in urban areas. For example, a compact urban form may make streets more walkable, reduce trip distances, and improve the share of public bus transport, thus reducing vehicle emissions and road dust (Ewing and Cervero, 2010). Increasing impervious surface areas in urban centers results in an increase in temperatures due to the urban heat island effect, which may contribute to the formation of air pollutants (Stone, 2008). High-density buildings may hinder the dispersion of air pollutants, leading to higher levels of pollutant accumulation (Hang et al., 2009).

Previous studies have thus far covered various perspectives. Some empirical studies compared average concentrations of air pollutants from ground-monitoring stations in different cities to analyze the effects of the urban built environment on air quality. For example, Bereitschaft and Debbage (2013) explored the relationship between urban form (street accessibility, degree of centering, land use mix, residential density, sprawl index, urban continuity, and shape complexity) and air pollution among 86 metropolitan areas in the United States, and the results show that cities with higher degrees of urban sprawl exhibited higher concentrations and emissions of air pollution. Rodríguez et al. (2016) used a dataset of 249 large urban zones across Europe and identified the determinants of air pollutant concentrations, and the results suggest that fragmented cities have higher levels of PM_{10}. Liu et al. (2016) examined the relationship between urban form and urban smog in 30 Chinese cities, and the results indicate that urban elongation and compactness are positively correlated to PM_{10}. Based on empirical data from 157 Chinese cities, Yuan et al. (2018) found that higher population density and lower urban continuity are usually associated with better air quality. In these studies, the urban areas of a city were taken as a single sample to evaluate its built environment, and spatial metrics for different parts of the city were overlooked.

With the development of urban simulation models, some studies have used “bottom-up” models to evaluate air pollution under different scenarios in a city. Marquez and Smith (1999) integrated land use, transportation, and airshed models to develop a framework for linking urban form and air quality. Subsequently, a series of modelling studies that integrate land-use models, transportation models, and emission models has been carried out to predict emissions based on specific land-use scenarios for individual cities. For example, a scenario analysis study in Xiamen, China, showed that compact development not only reduces vehicle emissions but also increases population-weighted exposures (Yuan et al., 2017). This is because a low-density scenario drives people away from high-pollution areas, while a high-density scenario places more people within such areas. However, air pollutants from emissions may disperse and interact with other factors (such as the urban heat island effect (Civerolo et al., 2007), and the street canyon effect (Buccolieri et al., 2010)), which can dynamically change air pollution concentrations. Hence, such “bottom-up” models do not adequately evaluate air pollution under different scenarios in a city.

Pollution ground-monitoring stations provide more data support and promote empirical studies on a single city. For example, Xu et al. (2016) used data from nine ground-monitoring stations to explore the quantitative relationship between land cover and air quality in Wuhan, China; the results show that land use categories (e.g., built-up land, vegetation, and water) have different effects on different air pollutants. Wu et al. (2015) further applied landscape metrics of different land covers (cropland, vegetation, water, and construction land) and examined the effect of urban landscape patterns on $PM_{2.5}$ concentrations as measured by monitoring sites in Beijing. Weber et al. (2014) revealed a positive correlation between PM_{10} concentrations and urban structures (including single and semi-detached houses, multi-story housing, and terraced houses) in Leipzig, Germany, but the PM_{10} data used in the air dispersion model were collected only from four ground-monitoring stations. In general, a limited number of ground-monitoring stations cannot provide detailed information for performing mathematical statistical analyses on $PM_{2.5}$ concentrations.

Overall, air pollution data from ground monitoring and “bottom-up” models in past studies are not sufficient to gain a deeper, more precise understanding of the association between the built environment and $PM_{2.5}$ concentration. Remote sensing techniques have become increasingly popular in recent years for monitoring $PM_{2.5}$ concentration (Geng et al., 2015; Li et al., 2017b). Compared with data from ground monitoring sites and “bottom-up” models used in past studies, the high resolution and wall-to-wall coverage data from remote sensing products could provide more support to examine the association between $PM_{2.5}$ concentration and built environments in urban areas.

Limited studies have used remote sensing data to explain the association. Therefore, the objective of this study is to use remote sensing technologies to derive a high spatial resolution (1 km*1 km) map of $PM_{2.5}$ concentrations, and explore the association between three different aspects of built environments (urban land cover, urban land use, and urban form) and $PM_{2.5}$ concentrations in urban areas. The study contributes to the literature by expanding the application of remote sensing in urban planning and development, and its novelty is that it expands the limited ground-monitoring data by providing a hundred samples of $PM_{2.5}$ concentrations in urban areas for statistical analyses on urban built environments.

2. Study area and data

Wuhan, the capital city of Hubei province, was selected for this study for several reasons: (1) According to the World Health Organization's Ambient Air Pollution Database 2016, Wuhan ranked 12th in terms of $PM_{2.5}$ concentrations among 210 Chinese cities, and $PM_{2.5}$ has become a significant environmental threat for its citizens. (2) Wuhan is nearly a thousand kilometers away from the Jingjinji Metropolitan Region (Beijing-Tianjin-Hebei), thus reducing any outside interference that this area with significant haze pollution problems would have on Wuhan. (3) Due to a significant increase in motor vehicles in recent years (from 1 million vehicles in 2010 to 2.7 million in 2017), transport-related emissions have become a major source of air pollution in Wuhan.

According to data from monitoring sites in Wuhan, the average concentration of $PM_{2.5}$ in 2016 was the highest in January, with the average value reaching approximately 104 $\mu g/m^3$ (the average value for 2016 was 57 $\mu g/m^3$). In January 2016, 74% of the days failed to meet the National Ambient Air Quality Standard (NAAQS) for $PM_{2.5}$ concentrations (75 $\mu g/m^3$). Uncovering association between the built environment and $PM_{2.5}$ concentrations during the period in which pollution levels were the highest may provide insights and their implications for urban planning. Therefore, January 2016 was selected as the study period. As Fig. 1 shows, the study area of central Wuhan covers approximately 550 km^2 with a population of

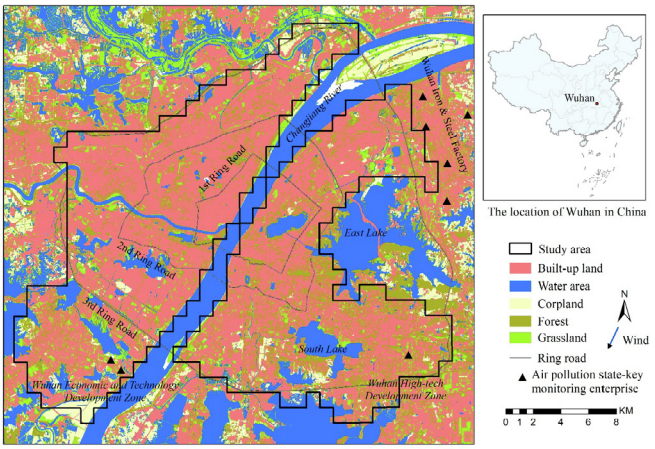

Fig. 1. Study area.

4.2 million people. Most polluting industries, such as the Wuhan Iron & Steel Factory zone, are excluded from the study area. These enterprises were forced by the government to reduce emissions or shut down during periods of severe haze pollution. The study area and period were designed to reduce any bias caused by industrial emissions on the results. Data used in this study include national ground monitoring data and Moderate Resolution Imaging Spectroradiometer (MODIS) remote sensing data for January 2016 and Geographic Information System (GIS) data on land use, roads, land cover, and buildings for 2014.

3. Methodology

As Fig. 2 shows, 1 km*1 km grids in Wuhan were selected as samples; $PM_{2.5}$ concentration distributions were estimated using a machine learning method; and three kinds of urban built environment metrics, namely land cover, land use, and urban form, were calculated. It was assumed that $PM_{2.5}$ concentration in a grid is correlated with both the built environment of the grid and the concentrations in the neighboring grids, and a spatial statistical analysis was carried out to explore the effects of urban built environment on $PM_{2.5}$ concentration.

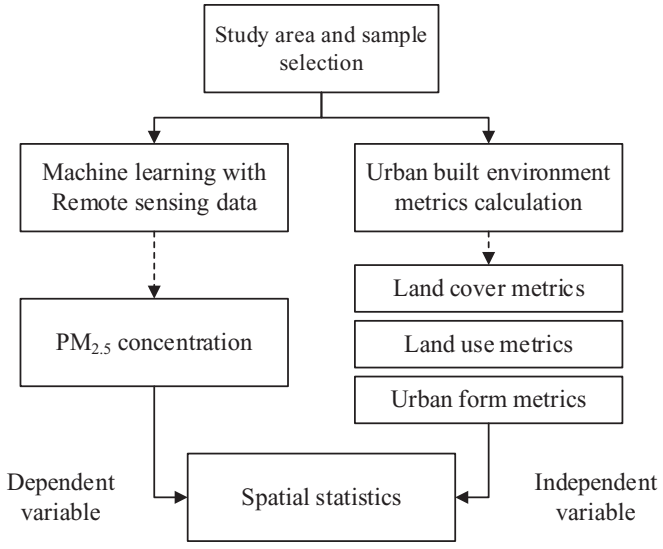

Fig. 2. Flowchart of the study.

3.1. Estimation of $PM_{2.5}$ concentrations

This study used a Deep Belief Network (DBN) to produce spatial distribution maps of the average $PM_{2.5}$ concentration in January 2016 in Wuhan urban agglomeration (Li et al., 2017a). The estimation of $PM_{2.5}$ concentration has been gradually considered a multivariable and non-linear problem, and the DBN has the potential to better represent the complex non-linear relationship (Li et al., 2017c). To be more specific, 1 km*1 km ground-level $PM_{2.5}$ was estimated with a DBN, containing a dependent variable ($PM_{2.5}$ concentration from air pollution monitoring stations) and two types of predictors (satellite observations and meteorological parameters). Satellite observations were obtained from MODIS products MYD02, MYD35, and MYD13 (a resolution of 1 km), and they included B1, B3, and B7 top-of-atmosphere (TOA) reflectance; observation angles; cloud mask; and normalized difference vegetation index (NDVI). Meteorological parameters included air temperature, surface pressure, wind speed, relative humidity, and planetary boundary layer height. A 10-fold cross-validation method was used to test for potential model overfitting and to estimate the predictive power of the sample. The results show that the mapped $PM_{2.5}$ distribution (1 km*1 km) retrieved from MODIS products is consistent with the site measurements, with the values of R^2 and RMSE reaching 0.87 and 9.89 $\mu g/m^3$, respectively. The study area includes 479 1 km*1 km grids in total, which was sufficient for the statistical analysis.

3.2. Metrics of the built environment

This study uses land cover, land use, and urban form to represent the built environment, and Fig. 3 shows an example of data for land cover, land use, buildings, and street networks.

Land cover is measured in terms of proportions of different land cover types in each grid area. In the study area, buildings account for 25% of the total area, forests 15%, grasslands 7%, roads 1%, and water 10%. This information on land cover was obtained from high resolution remote sensing data, and some of these land cover types could be further classified into sub-types. For example, low-rise high-density building areas account for most of the land area covered by buildings (38%), followed by high-rise high-density building areas (27%) and high-rise low-density building areas (22%).

The proportions of different land use types in each grid are used to reflect urban functions. In the study area, the land use types include residential land (R, 30%), business land (B, 5%), administration land (A, 11%), industrial land (M, 11%), and green and natural land (G, 5%). The study used Shannon's diversity index to measure the land use mix for each grid.

The study used data on buildings and street networks to measure urban form. For buildings, the building density, floor area ratio (FAR), and mean floor count were measured in each grid. For street network, the road density of different types of roads, road junction density, bus station density, and bus route density were measured in each grid. Streets were classified into four levels: express roads (14%), arterial roads (15%), sub-arterial roads (19%), and branch roads (52%).

Statistics for all variables are shown in Table 5.

3.3. Statistical methods

Spatial statistics have been used to evaluate the effect of natural and anthropogenic factors on haze pollution with a cross-section data of prefecture-level cities in China in previous studies (Hao and Liu, 2015; Liu et al., 2017). First, this study calculated a global autocorrelation index (Moran's I) using values for all the grids in the

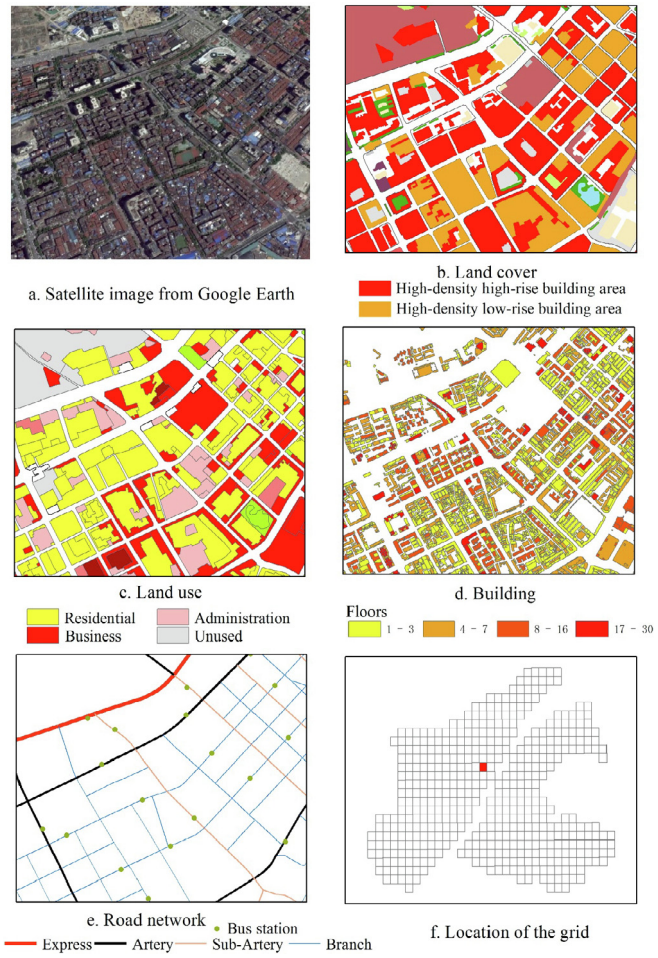

Fig. 3. Examples of data used to calculate metrics of the built environment.

study area to evaluate whether patterns of $PM_{2.5}$ concentrations are clustered, dispersed, or random. Moran's I ranges from −1 to 1, where positive values indicate spatial clustering, negative values indicate spatial dispersion, and zero indicates no spatial autocorrelation. The study further used Anselin Local Moran's I (LISA) to show the relationship of $PM_{2.5}$ concentrations between each grid and its surrounding grids across the study area. The spatial pattern of LISA can help locate areas with clusters of high $PM_{2.5}$ concentrations (HH) and areas with clusters of low $PM_{2.5}$ concentrations (LL). The study used a Queen contiguity weights matrix for the spatial autocorrelation analysis.

If significant spatial autocorrelation is detected, it indicates that $PM_{2.5}$ concentrations in individual grids may be associated with or even dependent on the neighboring grids. Traditional statistical methods, such as the Pearson correlation, cannot be used to explore cases with spatial autocorrelation (Anselin, 1988; Wan and Su, 2016). Spatial statistics, namely spatial lag models (SLM, Eq. (1)) and spatial error models (SEM, Eq. (2)), are used to explore correlations between the built environment and $PM_{2.5}$ concentrations, and robust Lagrange multiplier tests are used to select a specific model (Su et al., 2017). All variables have been standardized before performing statistical analyses, and all modelling was performed using GeoDa software.

$$Y = a + bX + \lambda W_Y + e \quad (1)$$

$$Y = a + bX + e \ (e = \lambda W_e + u) \quad (2)$$

In these equations, Y represents the $PM_{2.5}$ concentrations for each grid; X represents metrics associated with the built environment; e is the error term; λ is the spatial autoregressive coefficient; W_Y and W_e are the spatial matrices for Y and e, respectively; and a and u are the scalar variables.

4. Results

4.1. Spatial patterns of $PM_{2.5}$ concentrations

In the study area, $PM_{2.5}$ concentrations ranged from 87 to 116 μg/m^3 with a mean value of 94 μg/m^3. All grids had an average value above 1.5 times the national standard. As Fig. 4 shows, the area within the first ring road had the highest level of $PM_{2.5}$ concentrations ranging from 97 to 116 μg/m^3; this region was considered a high-high cluster by LISA analysis. Grids with the lowest level of $PM_{2.5}$ concentrations were located at the south-eastern corner of the third ring road (low-low clusters), which is near the Wuhan East Lake High-Tech Development Zone. With the exception of areas in the north-eastern corner of the third ring road (a high-high cluster), the area between the second and third ring roads exhibited medium levels of air pollution with values ranging from 96 to 104 μg/m^3. In the entire study area, there was only one grid with a high level of $PM_{2.5}$ concentrations surrounded by low levels of pollution (a high-low outlier).

The global Moran's I for the study area was 0.57 ($p < 0.001$), which indicates that spatial autocorrelation for $PM_{2.5}$ concentrations across all grids is a significant problem. In terms of statistics, this violates the assumption of independent observations, and using the Pearson correlation would be inappropriate (Haining and Zhang, 2003). More importantly, air pollution in one grid may be generated by vehicles passing across the neighboring girds. The built environment can influence not only influence $PM_{2.5}$ concentrations in its own grid but also the air quality of the neighboring grids. Thus, it is necessary to use spatial statistics to explore the association between air pollution and the built environment.

4.2. Association between land cover and $PM_{2.5}$ concentrations

The results of the spatial statistics and spatial patterns of land covers are shown in Table 1 and Fig. 5, respectively. The spatial autoregressive coefficients λ was significantly positive in all models, which once again verifies the spatial autocorrelation of $PM_{2.5}$ concentrations. Unexpectedly, the proportion of forest area within a grid is not correlated to $PM_{2.5}$ concentrations. This may be due to the dormancy of trees during winter decreasing $PM_{2.5}$ absorption, especially for deciduous trees. The proportion of grasslands in a grid is both significantly and negatively correlated to

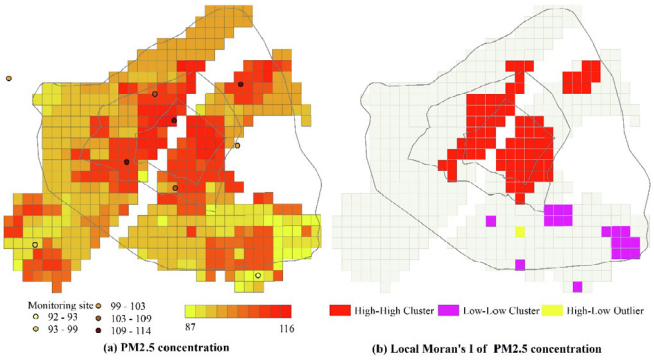

Fig. 4. $PM_{2.5}$ concentrations and spatial autocorrelation analysis.

Table 1
Correlation between land cover and $PM_{2.5}$ concentration.

ID	Metric	B	P	Model	LM lag	Robust LM lag	LM error	Robust LM error
1	λ r_Forest	**0.81**	**0**	SLM	0	0.991	0	0.668
		0.023	0.443					
2	λ r_Grass	**0.79**	**0**	SLM	0	0	0	0.102
		−0.075	**0.014**					
3	λ r_ForeGrass	**0.81**	**0**	SLM	0	0	0	0.162
		−0.023	0.442					
4	λ r_Building	**0.79**	**0**	SLM	0	0	0	0.687
		0.091	**0.003**					
5	λ r_HBuildA	**0.78**	**0**	SLM	0	0	0	0.342
		0.092	**0.003**					
6	λ r_LBuildA	**0.81**	**0**	SEM	0	0.689	0	0.183
		0.071	**0.053**					
7	λ r_HSBuild	**0.81**	**0**	SLM	0	0.015	0	0.32
		−0.004	0.88					
8	λ r_LSBuild	**0.81**	**0**	SLM	0	0.001	0	0.77
		−0.045	0.13					
9	λ r_HHBuildA	**0.75**	**0**	SLM	0	0	0	0.591
		0.13	**0**					
10	λ r_LHBuildA	**0.81**	**0**	SLM	0	0.02	0	0.408
		0.012	0.689					
11	λ r_Water	**0.81**	**0**	SLM	0	0.484	0	0.686
		0.0008	0.97					
12	λ r_Construction	**0.81**	**0**	SLM	0	0.002	0	0.788
		−0.05	0.1					

Note: bolded values indicate metrics statistically significant at $P < 0.1$ level.

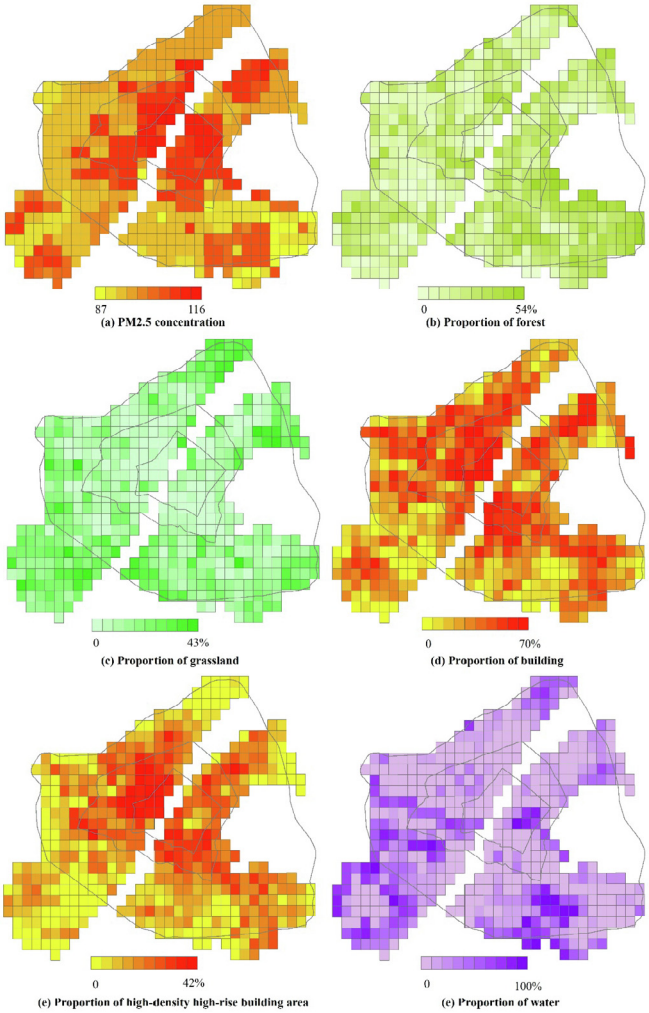

Fig. 5. Proportion of different land covers.

$PM_{2.5}$ concentrations, with the correlation becoming insignificant when proportions of forests and grasslands are added. Grasslands provide open space to disperse pollution, and evergreen shrubs can exhibit the positive effect of absorbing $PM_{2.5}$ in winter (Liang et al., 2014). Air pollution over some lakes, such as South Lake and East Lake, is relatively high, and the proportion of water in a grid is not significantly related to $PM_{2.5}$ concentrations. On the one hand, open spaces over lakes help to disperse air pollution; however, higher humidity over lakes can intensify the formation of $PM_{2.5}$ (Cheng et al., 2015).

The proportion of building areas within a grid is both significantly and positively correlated with $PM_{2.5}$ concentrations, and the study further analyzed whether building types affected $PM_{2.5}$ concentrations. Compared with separate buildings (r_HSBuild, r_LSBuild), building areas (r_HBuildA, r_LBuildA) usually have a significant correlation with air quality. High-rise, high-density building areas have the largest impact on $PM_{2.5}$ concentrations ($B = 0.13$, $P = 0$). Although building construction is a source of haze in urban areas, the proportion of construction sites within a grid is not related to $PM_{2.5}$ concentrations. This is likely due to the emergency procedures dictated by the government during haze emergencies, during which construction of buildings is halted, thus temporarily limiting the impact of construction on $PM_{2.5}$ concentrations.

4.3. Association between land use and $PM_{2.5}$ concentrations

The results from the spatial statistics and the spatial patterns of land uses are illustrated in Table 2 and Fig. 6, respectively. Residential lands account for the largest portion of the study area, and their proportion is significantly correlated to $PM_{2.5}$ concentrations. This suggests a high risk of exposure to air pollution for urban residents, especially for the elderly and children who spend most of their time at home. The proportion of administration land is less but significantly correlated to $PM_{2.5}$ concentrations. Somewhat surprisingly, the proportion of industrial land in a grid is negatively associated with air pollution. The geographical location of the national key monitoring pollution sources was overlapped with the

Table 2
Correlation between land use and $PM_{2.5}$ concentration.

ID	Metric	B	P	Model	LM lag	Robust LM lag	LM error	Robust LM error
1	λ r_R	**0.78**	**0**	SLM	0	0	0	0.733
		0.098	**0.001**					
2	λ r_A	**0.81**	**0**	SLM	0	0.034	0	0.362
		0.063	**0.04**					
3	λ r_B	**0.82**	**0**	SLM	0	0	0	0.029
		0.044	0.15					
4	λ r_M	**0.79**	**0**	SLM	0	0	0	0.397
		−0.097	**0.001**					
5	λ r_G	**0.81**	**0**	SLM	0	0.021	0	0.202
		−0.001	0.97					
6	λ Shanon	**0.81**	**0**	SLM	0	0	0	0.08
		0.008	0.79					

Note: bolded values indicate metrics statistically significant at $P < 0.1$ level.

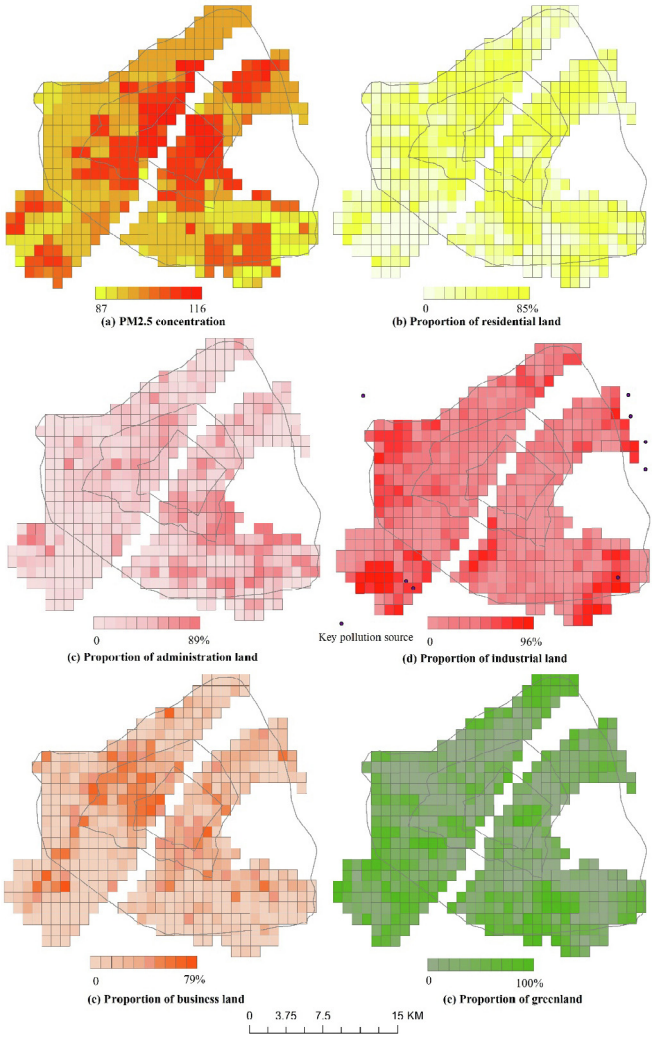

Fig. 6. Proportion of different land uses.

map of industrial land (Fig. 6 d), and most of industrial pollution sources were found to be outside downtown Wuhan. Industrial lands are mainly located in Wuhan Economic and Technological Development Zone, and most of enterprises (automobile, electronics and electrical appliances, etc.) are non-polluting industries. As the Shannon diversity index shows, land use mix is not significantly associated with air quality; this result is shared by another empirical study that utilized points of interest (POI) data in China (Yuan et al., 2018). Although a higher degree of land use mix may reduce travelling distances for residents, it may also increase traffic disorder that leads to increased emissions (Ding, 2009).

4.4. Association between urban form and $PM_{2.5}$ concentrations

The results of spatial statistics and spatial patterns of urban form are illustrated in Table 3 and Fig. 7 respectively. Grids with higher values of FAR are most commonly located within the second ring road, and FAR is significantly correlated to the levels of $PM_{2.5}$ concentrations. A higher value of FAR indicates a higher level of population density within a grid, and these areas account for a larger portion of traffic sources and associated vehicle emissions. Building density is also positively correlated to $PM_{2.5}$ concentrations, but mean floor count is unrelated to the levels of air pollution. This suggests that building density has a larger impact on air ventilation than building height. These results are generally consistent with the analysis in Section 5.2, which indicates that high-rise high-density building areas have a large influence on $PM_{2.5}$ concentrations.

Road density for all types of roads is significantly correlated to $PM_{2.5}$ concentrations, but the correlation varies with different types of roads. There is a significant correlation between $PM_{2.5}$ concentrations and the densities of arterial roads and sub-arterial roads, but the densities of express and branch roads are unrelated to $PM_{2.5}$ concentrations. This may be due to the opposite effects of traffic volume and traffic speed on vehicle emissions. Greater volumes of traffic produce more air pollution, and lower driving speeds may increase rates of tailpipe emissions (Wang et al., 2014). As Model 10 shows, road junction density has a positive impact on $PM_{2.5}$ concentrations because more road junctions may reduce driving speeds and increase the number of stops in a trip. Although express roads are loaded with large traffic volumes, these roads have more overpasses and fewer road junctions, leading to higher driving speeds and lower emission rates. Branch roads generally bear smaller traffic volumes; as such, their influence on $PM_{2.5}$ concentrations is not obvious.

5. Discussions and implications

The results show that areas with a high density of buildings are associated with much higher $PM_{2.5}$ exposure levels than those with less density. These areas with crowded populations are major sources of vehicle emissions, and people in these areas are also subjected to higher levels of $PM_{2.5}$ exposures. The dispersion and dilution of $PM_{2.5}$ partly depends on weather conditions, especially on wind direction and velocity, and so an increase in building

Table 3
Correlation between urban form and $PM_{2.5}$ concentration.

ID	Metric	B	P	Model	LM lag	Robust LM lag	LM error	Robust LM error
1	λ D_Build	**0.79**	**0**	SLM	0	0	0	0.784
		0.083	**0.007**					
2	λ FAR	**0.77**	**0**	SLM	0	0	0	0.741
		0.107	**0.001**					
3	λ Floor	**0.81**	**0**	SLM	0	0	0	0.007
		0.005	0.857					
4	λ D_RoadAll	**0.79**	**0**	SLM	0	0	0	0.018
		0.059	**0.053**					
5	λ D_Express	**0.81**	**0**	SEM	0	0.274	0	0.099
		−0.026	0.4					
6	λ D_Artery	**0.77**	**0**	SLM	0	0	0	0.81
		0.102	**0**					
7	λ D_SubArtery	**0.78**	**0**	SLM	0	0.01	0	0.371
		0.1	**0**					
8	λ D_Brach	**0.8**	**0**	SLM	0	0	0	0.025
		0.036	0.24					
9	λ D_Junction	**0.78**	**0**	SLM	0	0	0	0.019
		0.077	**0.012**					

Note: bolded values indicate metrics statistically significant at $P < 0.1$ level.

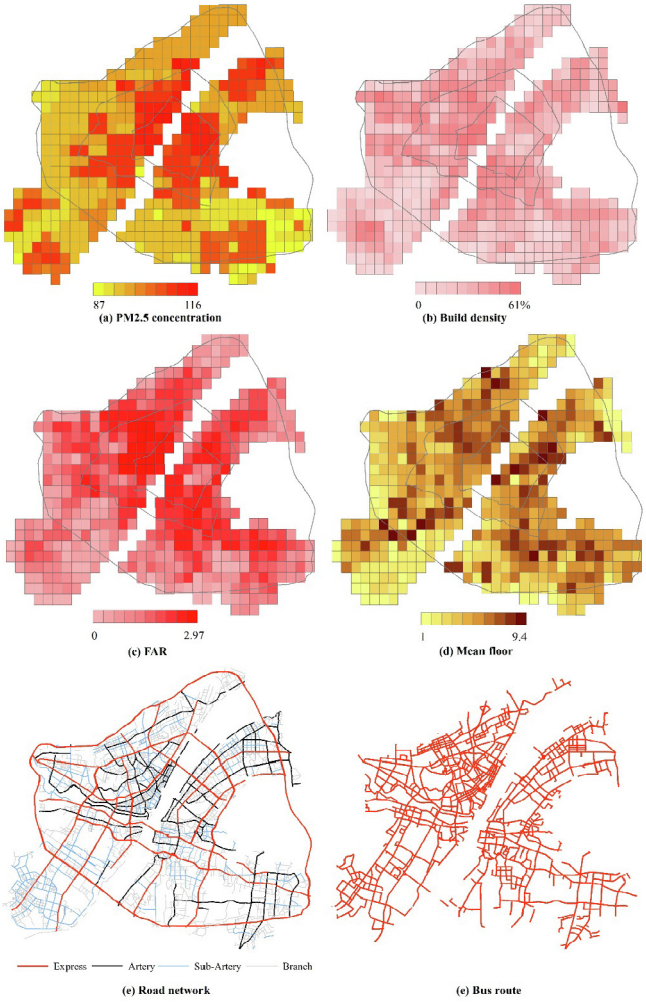

Fig. 7. Spatial patterns of urban form metrics.

density will lead to a decrease ventilation and PM2.5 dispersion. It is necessary to properly manage building density in Chinese megacities; a polycentric urban form may help to balance high population density in downtown areas and to reduce traffic emissions and exposure to air pollution.

The spatial patterns of street canyons may also influence pollution dispersion. To study this, the pollution levels in two neighboring grids were analyzed (Fig. 8). Although Grid B has higher values for building density and road density than Grid A, the $PM_{2.5}$ concentrations of Grid B are lower than those of Grid A. Streets that are parallel to the main wind direction (Grid B) may increase pollution dispersion. On the contrary, streets that are perpendicular to the main wind direction (Grid A) may decrease the pollution dispersion, and a higher wind speed may stir up dust and lead to increased levels of $PM_{2.5}$ concentrations. This implies that the spatial morphology of blocks is as important to improving air quality as the urban form metrics, such as building density, discussed in this study. Since buildings are already quite dense in Chinese cities (Huang et al., 2007), the spatial patterns of street canyons should be considered during urban design and urban renewal, especially for older towns.

Previous studies have showed the association between landscape metrics and air pollution (Wu et al., 2015). In this study, the

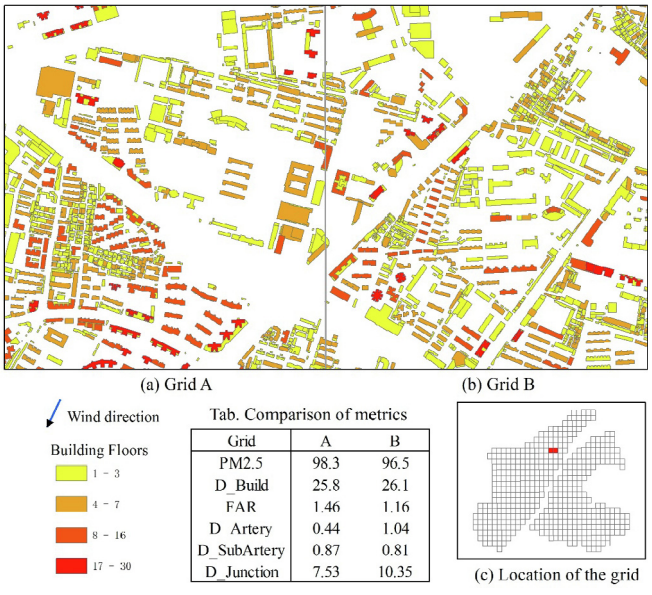

Fig. 8. Comparison of urban form.

Table 4
Analysis for SHAPE of buildings, road and public transport.

ID	Metric	B	P	Model	LM lag	Robust LM lag	LM error	Robust LM error
1	λ	0.78	0	SLM	0	0	0	0.91
	D_Build	**0.096**	**0.002**					
	SHAPE_Build	**0.059**	**0.057**					
2	λ	**0.8**	**0**	SLM	0	0	0	0.027
	r_Road	0.047	0.148					
	ED_Road	**−0.062**	**0.054**					
3	λ	**0.76**	**0**	SLM	0	0	0	0.905
	FAR	**0.113**	**0.016**					
	D_Station	**−0.095**	**0.023**					
	D_Route	**0.0853**	**0.051**					

Area Weighted Mean Shape Index (SHAPE), which is equal to the area weighted result of the building perimeter divided by the square root of the base area, is used to measure the spatial form of buildings and to evaluate the correlation between $PM_{2.5}$ concentrations and SHAPE values. As Table 4 shows, an increase in the SHAPE value of buildings increases $PM_{2.5}$ concentrations, and so building morphology may play a significant role in the dispersion of pollutants around buildings. This indicates that tower-type buildings (buildings with smaller SHAPE values) may have a greater effect on pollution dispersion than slab-type buildings (buildings with larger SHAPE values).

The impact of roads on $PM_{2.5}$ concentrations depends on traffic volumes and driving speeds associated with different road types, and reducing traffic jams can help to improve air quality. The negative relationship between $PM_{2.5}$ concentrations and edge density (ED) of roads (Model 2 in Table 4) shows the importance of road levels. In case of same road areas, blocks with low-level roads usually have higher values of edge density than blocks with high-level roads. This result supports the view of transition from "large blocks and wide roads" mode to "small blocks and narrow roads" mode in Chinses cities. To illustrate this, two neighboring grids were selected and compared to find the difference between large blocks (Grid A) and small blocks (Grid B) in Fig. 9. Although Grid B has higher values for building densities, FAR, and road density than Grid A, concentrations of $PM_{2.5}$ are nearly identical for both the grids. It should also be noted that the wind path in Grid B may improve pollutant dispersion, and further research with field observation data would be beneficial to explain the effects of "small blocks and narrow roads"-style development on air pollution.

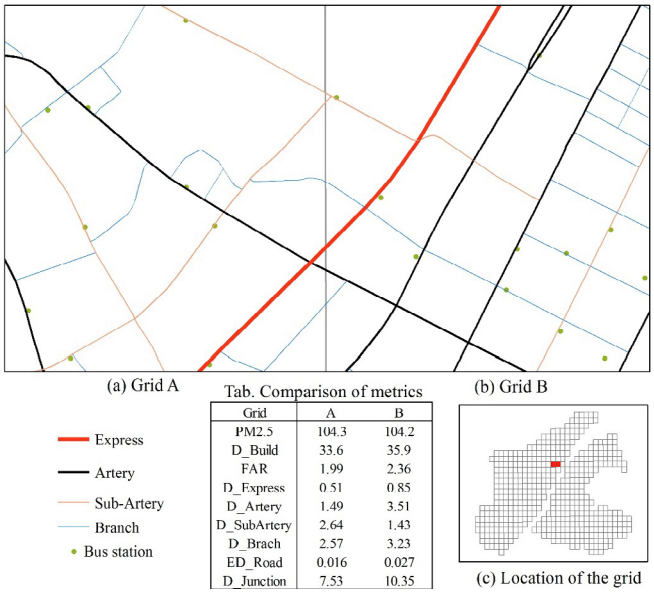

Fig. 9. Comparison between a large block and a small block.

The correlation between $PM_{2.5}$ concentrations and public transportation after controlling for FAR (which represents travel demand) is shown in Model 3. Bus station density has a negative influence on $PM_{2.5}$ concentrations, which shows that improving access to public transportation may decrease the share of private cars. Bus route density (km/km^2) is positively correlated to $PM_{2.5}$ concentrations. This may be due to a high value of bus route overlapping factor in the study area (rate of total route length to total road length, suitable value: 1.25–2.5, Wuhan: 4.05), which may lead to traffic jams and more emissions. This suggests that bus networks should be optimized simultaneously with road networks.

Unexpectedly, the analysis show that forests do not lead to a reduction in haze. This may be due to dormancy of trees in winter, and more evergreen trees, such as Cedrus deodara, could be planted (Wang et al., 2015). Another potential explanation for this phenomenon can be that the grids with higher levels of forest area and $PM_{2.5}$ concentrations are located near sources of pollution. Grids with high levels of forests are generally located to the south of East Lake (Fig. 5b), and forests in these grids are affected by pollution generated from the northeast, such as the Wuhan Iron & Steel Factory Zone, which disperses across East Lake. To further evaluate the ability of forests to mitigate pollution, the study compared $PM_{2.5}$ concentrations between these grids and each of the neighboring grids in downwind direction one by one. The results show that concentrations of $PM_{2.5}$ in grids that are downwind are much lower than those in grids that are upwind, with a mean difference value of 7.5 $\mu g/m^3$. This shows the ability of forests to absorb $PM_{2.5}$.

The limitations of this study could be addressed in future research. The study only considered $PM_{2.5}$ concentrations in January; the spatial pattern of $PM_{2.5}$ concentrations may change due to a variety of environmental factors such as weather or increased tree activity in other months. As such, the association between the built environment and air pollution should be explored for the entire year. This study primarily explores the correlations between metrics of the built environment and $PM_{2.5}$ concentrations, and more advanced models can be used to explore the interactions between different metrics of the built environment. The effect of wind direction and speed should be included in future spatial models, as these environmental factors may affect concentrations of air pollution. Maps of $PM_{2.5}$ concentrations (1 km*1 km, $R^2 = 0.87$, RMSE = 9.89 $\mu g/m^3$) were retrieved from the DBN coupled with MODIS products, and future studies may use newly launched satellites data (such as high-resolution satellite observations and satellite with atmospheric parameters) to improve the accuracy of $PM_{2.5}$ concentrations.

6. Conclusions

$PM_{2.5}$ pollution has created a great threat to public health in

Table 5
Statistics of all the variables.

Category	Metrics	Min	Max	Mean	Std.D	Note
$PM_{2.5}$ concentration		87.41	116.45	93.72	4.73	
Land cover (%)	r_Building	0	68.94	25.2	14.66	
	r_Forest	0	53.71	14.86	9.36	
	r_Grass	0	42.82	7.53	6.9	
	r_ForeGrass	0	62.47	22.39	11.55	Sum of forest and grassland
	r_HBuildA	0	52	12.51	11.71	High-rise building area
	r_LBuildA	0	45.65	10.19	8.72	Low-rise building area
	r_HSBuild	0	7	1.49	1.43	High-rise separate building
	r_LSBuild	0	22.77	1.01	1.42	Low-rise separate building
	r_HHBuildA	0	42	6.91	7.98	High-rise high-density building area
	r_LHBuildA	0	37	5.6	7.21	High-rise low-density building area
	r_Construction	0	87.05	13.58	13.9	Construction site
	r_Water	0	99.83	9.59	17.05	
Land use (%)	r_R	0	85.14	30.26	21.26	Residential land
	r_A	0	89.28	11.35	16.22	Administration land
	r_B	0	79	4.49	6.97	Business land
	r_M	0	96.36	10.91	16.72	Industrial land
	r_G	0	99.84	22.2	23.72	Green land
	Shanon	0	1.33	0.71	0.34	Land use mix
Building	FAR	0	2.98	0.78	0.58	
	Floor	1	9.42	3.16	1.41	Mean floor
	D_Build	0.01	60.51	18.27	10.78	Building density (%)
Street network	D_Express	0	2.87	0.52	0.61	Express road density (km/km^2)
	D_Artery	0	4	0.58	0.75	Arterial road density (km/km^2)
	D_SubArtery	0	4	0.68	0.8	Sub-arterial road density (km/km^2)
	D_Brach	0	8	1.92	1.35	Branch road density (km/km^2)
	D_RoadAll	0	13.17	3.7	1.91	Road Density for all type (km/km^2)
	D_Junction	0	55.48	8	6.83	Road junction

Note: separate building: building density<10%, building area: building density>10%, high-density building area: building density>50%, low-density building area: building density<50%, high-rise building: floor>4, low-rise building: floor<4.

China, and more attention should be paid to the built environment in Chinese cities. Past studies were usually dependent on limited ground-monitoring data (about 10 or less ground-monitoring stations), which are not sufficient to explore the association between built environment and $PM_{2.5}$ concentration. To fill up the knowledge gap, the study used remote sensing technologies to expand limited ground-monitoring data by selecting about 500 grids of $PM_{2.5}$ concentrations in downtown Wuhan, and exploring the correlation between the concentration and land cover, land use, and urban form using spatial statistics. For land cover, high-rise high-density building areas have the largest impact on $PM_{2.5}$ concentrations, and the effect of forestland is not obvious in winter. For land use, industrial lands in the downtown are unrelated to air pollution, and transportation has become a main source of $PM_{2.5}$ pollution. For urban form, FAR and building density are positively associated with $PM_{2.5}$ concentrations, and different types of road densities have different effects on air pollution. The implications of the study for urban planning and development are given at last. High-density development areas are correlated with higher levels of $PM_{2.5}$ pollution, and building density and FAR are extremely high in downtown Wuhan. To deal with this challenge, it is necessary for urban planners to develop a polycentric urban structure to balance high population density and to reduce traffic emissions in downtown areas. Road and bus networks should be optimized simultaneously to reduce traffic jams, and more public transits (such as subways) should be built to link urban sub-centers to the downtown. The spatial morphology of streets and buildings should be considered during urban design and urban renewal, and "small blocks and narrow roads" may be considered an alternative for urban development. More forestlands should be allocated near industrial pollution sources, and more evergreen trees should be planted in downtown Wuhan. In general, the study contributes to the application of remote sensing in urban planning and development, and remotely sensed $PM_{2.5}$ concentration data could provide more findings and implications than air pollution data obtained from ground monitoring and "bottom-up" models in past studies.

Funding

This research was funded by National Natural Science Foundation of China (grant: 51708234, 51678259, 51708233).

References

Anselin, L., 1988. Spatial Econometrics: Methods and Models. Springer, Netherlands.
Bereitschaft, B., Debbage, K., 2013. Urban form, air pollution, and CO2 emissions in large US metropolitan areas. Prof. Geogr. 65 (4), 612–635.
Buccolieri, R., Sandberg, M., Di Sabatino, S., 2010. City breathability and its link to pollutant concentration distribution within urban-like geometries. Atmos. Environ. 44 (15), 1894–1903.
Cao, G., Zhang, X., Gong, S., An, X., Wang, Y., 2011. Emission inventories of primary particles and pollutant gases for China. Chin. Sci. Bull. 56 (8), 781–788.
Chen, X., Shao, S., Tian, Z., Xie, Z., Yin, P., 2017. Impacts of air pollution and its spatial spillover effect on public health based on China's big data sample. J. Clean. Prod. 142, 915–925.
Cheng, Y., He, K.B., Du, Z.Y., Zheng, M., Duan, F.K., Ma, Y.L., 2015. Humidity plays an important role in the PM 2.5 pollution in Beijing. Environ. Pollut. 197, 68–75.
Civerolo, K., Hogrefe, C., Lynn, B., Rosenthal, J., Ku, J.-Y., Solecki, W., Cox, J., Small, C., Rosenzweig, C., Goldberg, R., 2007. Estimating the effects of increased urbanization on surface meteorology and ozone concentrations in the New York City metropolitan region. Atmos. Environ. 41 (9), 1803–1818.
Ding, C., 2009. Growth, structure, and efficiency: assessment of spatial development patterns in Chinese cities. Planners 24 (12), 35–39.
Dominici, F., Peng, R.D., Bell, M.L., Pham, L., McDermott, A., Zeger, S.L., Samet, J.M., 2006. Fine particulate air pollution and hospital admission for cardiovascular and respiratory diseases. Jama 295 (10), 1127–1134.
Ewing, R., Cervero, R., 2010. Travel and the built environment: a meta-analysis. J. Am. Plann. Assoc. 76 (3), 265–294.
Fu, H., Chen, J., 2017. Formation, features and controlling strategies of severe haze-fog pollution in China. Sci. Total Environ. 578, 121–138.
Geng, G., Zhang, Q., Martin, R.V., Donkelaar, A.V., Huo, H., Che, H., Lin, J., He, K., 2015. Estimating long-term PM 2.5 concentrations in China using satellite-based aerosol optical depth and a chemical transport model. Rem. Sens. Environ. 166, 262–270.
Haining, R., Zhang, J., 2003. Spatial Data Analysis: Theory and Practice. Cambridge University Press.

Han, X., Liu, Y., Gao, H., Ma, J., Mao, X., Wang, Y., Ma, X., 2017. Forecasting PM2.5 induced male lung cancer morbidity in China using satellite retrieved PM2.5 and spatial analysis. Sci. Total Environ. 607–608, 1009–1017.
Hang, J., Sandberg, M., Li, Y., Claesson, L., 2009. Pollutant dispersion in idealized city models with different urban morphologies. Atmos. Environ. 43 (38), 6011–6025.
Hao, Y., Liu, Y.M., 2015. The influential factors of urban PM 2.5 concentrations in China: aspatial econometric analysis. J. Clean. Prod. 112, 1443–1453.
Huang, J., Lu, X., Sellers, J.M., 2007. A global comparative analysis of urban form: applying spatial metrics and remote sensing. Landsc. Urban Plann. 82 (4), 184–197.
Laden, F., Schwartz, J., Speizer, F.E., Dockery, D.W., 2006. Reduction in fine particulate air pollution and mortality: extended follow-up of the Harvard Six Cities study. Am. J. Respir. Crit. Care Med. 173 (6), 667–672.
Li, T., Shen, H., Yuan, Q., Zhang, L., 2017a. A Novel Solution for Remote Sensing of Air Quality: from Satellite Reflectance to Ground PM2.5. 1709.05912.
Li, T., Shen, H., Yuan, Q., Zhang, X., Zhang, L., 2017b. Estimating ground-level PM2.5 by fusing satellite and station observations: a geo-intelligent Deep learning approach. Geophys. Res. Lett. 44 (23), 11,985–11,993.
Li, T., Shen, H., Zeng, C., Yuan, Q., Zhang, L., 2017c. Point-surface fusion of station measurements and satellite observations for mapping PM 2.5 distribution in China: methods and assessment. Atmos. Environ. 152, 477–489.
Liang, D., Wang, B., Wang, Y., Zhang, H., Yang, S., Li, A., 2014. Ability of typical greenery shrubs of beijing to adsorb and arrest PM2.5. Environ. Sci. (9), 3605–3611.
Liu, H., Fang, C., Zhang, X., Wang, Z., Bao, C., Li, F., 2017. The effect of natural and anthropogenic factors on haze pollution in Chinese cities: a spatial econometrics approach. J. Clean. Prod. 165.
Liu, H., He, K., 2012. Traffic optimization: a new way for air pollution control in China's Urban Areas. Environ. Sci. Technol. 46 (11), 5660–5661.
Liu, Y., Arp, H.P.H., Song, X., Song, Y., 2016. Research on the relationship between urban form and urban smog in China. Environ. Plan. Plan. Des. 0 (0), 1–15.
Marquez, L.O., Smith, N.C., 1999. A framework for linking urban form and air quality. Environ. Model. Softw 14 (6), 541–548.
Pui, D.Y.H., Chen, S.C., Zuo, Z., 2014. PM2.5 in China: measurements, sources, visibility and health effects, and mitigation. 颗粒学报(Particuology) 13 (2), 1–26.
Rodríguez, M.C., Dupont-Courtade, L., Oueslati, W., 2016. Air pollution and urban structure linkages: evidence from European cities. Renew. Sustain. Energy Rev. 53 (1), 1–9.
Shi, Y., Matsunaga, T., Yamaguchi, Y., Li, Z., Gu, X., Chen, X., 2018. Long-term trends and spatial patterns of satellite-retrieved PM 2.5 concentrations in South and Southeast Asia from 1999 to 2014. Sci. Total Environ. 615, 177–186.
Stone, B., 2008. Urban sprawl and air quality in large US cities. J. Environ. Manag. 86 (4), 688–698.
Su, S., Pi, J., Xie, H., Cai, Z., Weng, M., 2017. Community deprivation, walkability, and public health: highlighting the social inequalities in land use planning for health promotion. Land Use Pol. 67, 315–326.
Wan, C., Su, S., 2016. Neighborhood housing deprivation and public health: theoretical linkage, empirical evidence, and implications for urban planning. Habitat Int. 57, 11–23.
Wang, B., Zhang, W., Niu, X., Wang, X., 2015. Particulate matter adsorption capacity of 10 evergreen species in beijing. Environ. Sci. (2), 408–414.
Wang, X., Liu, C., Kostyniuk, L., Shen, Q., Bao, S., 2014. The influence of street environments on fuel efficiency: insights from naturalistic driving. Int. J. Environ. Sci. Technol. 11 (8), 2291–2306.
Wang, Y., Yao, L., Wang, L., Liu, Z., Ji, D., Tang, G., Zhang, J., Sun, Y., Hu, B., Xin, J., 2014. Mechanism for the formation of the January 2013 heavy haze pollution episode over central and eastern China. Sci. China Earth Sci. 57 (1), 14–25.
Weber, N., Haase, D., Franck, U., 2014. Assessing modelled outdoor traffic-induced noise and air pollution around urban structures using the concept of landscape metrics. Landsc. Urban Plann. 125 (6), 105–116.
Wu, J., Xie, W., Li, W., Li, J., 2015. Effects of urban landscape pattern on PM2.5 pollution-A beijing case study. PLoS One 10 (11), e0142449.
Xu, G., Jiao, L., Zhao, S., Yuan, M., Li, X., Han, Y., Zhang, B., Dong, T., 2016. Examining the impacts of land use on air quality from a spatio-temporal perspective in Wuhan, China. Atmosphere 7 (5), 62.
Yuan, M., Song, Y., Hong, S., Huang, Y., 2017. Evaluating the effects of compact growth on air quality in already-high-density cities with an integrated land use-transport-emission model: a case study of Xiamen, China. Habitat Int. 69, 37–47.
Yuan, M., Song, Y., Huang, Y., Hong, S., Huang, L., 2018. Exploring the association between urban form and air quality in China. J. Plann. Educ. Res. 48 (4), 413–426.